

University of Dundee

G-PFEM Numerical Assessment of Screw Pile Undrained Capacity

Monforte, L.; Arroyo, Marcos; Gens, Antonio; Ciantia, Matteo

Published in:
ISSPEA 2019:

DOI:
[10.20933/100001123](https://doi.org/10.20933/100001123)

Publication date:
2019

Document Version
Peer reviewed version

[Link to publication in Discovery Research Portal](#)

Citation for published version (APA):

Monforte, L., Arroyo, M., Gens, A., & Ciantia, M. (2019). G-PFEM Numerical Assessment of Screw Pile Undrained Capacity. In C. Davidson, M. J. Brown, J. A. Knappett, A. J. Brennan, C. Augarde, W. Coombs, L. Wang, D. Richards, D. White, & A. Blake (Eds.), *ISSPEA 2019: 1st International Symposium on Screw Piles for Energy Applications* (pp. 95-100). University of Dundee. <https://doi.org/10.20933/100001123>

General rights

Copyright and moral rights for the publications made accessible in Discovery Research Portal are retained by the authors and/or other copyright owners and it is a condition of accessing publications that users recognise and abide by the legal requirements associated with these rights.

- Users may download and print one copy of any publication from Discovery Research Portal for the purpose of private study or research.
- You may not further distribute the material or use it for any profit-making activity or commercial gain.
- You may freely distribute the URL identifying the publication in the public portal.

Take down policy

If you believe that this document breaches copyright please contact us providing details, and we will remove access to the work immediately and investigate your claim.

G-PFEM NUMERICAL ASSESSMENT OF SCREW PILE UNDRAINED CAPACITY

L MONFORTE, M ARROYO and A GENS

Universitat Politècnica de Catalunya (UPC), Barcelona (Spain) - Department
of Civil and Environmental Engineering
lluis.monforte@upc.edu

M O CIANTIA

School of Science and Engineering, University of Dundee

SUMMARY: This contribution describes a preliminary parametric analysis of the factors affecting the pull-out resistance of screw-piles in undrained conditions. The numerical simulations rely on the Particle Finite Element method, a method known for its capabilities to tackle large deformations and rapid changing boundaries at large strains. A total stress analysis –assuming a quasi-incompressible elastic model along with a Tresca plastic model- is used to simulate the clayey soil behavior. Contact constraints are imposed to the solution with a penalty approach. As a first step, a two-dimensional geometry is used and the pile resistance to pullout and penetration is assessed.

INTRODUCTION

The fast growth of off-shore developments poses new challenges and increases the demand for cost-effective and reliable foundation solutions. Screw piles (or helical piles) have been proposed as a potential innovative alternative foundation in offshore environments. This kind of foundation is capable supporting large uplift loads. Examples of its application include the support of pipelines and the foundations for transmission towers^{1,2}.

The optimization of the geometry of the screw pile has been historically addressed by experimental means and also through the use of quite simplified analytical solutions. Although much insight is gained from such analyses, a number of basic features of the problem are left aside. Consequently, nowadays, numerical models are predominant. The Finite Element method (FEM) allows to accurately simulate the non-linear behavior of clayey soils using well-honed tools of continuum mechanics (field equations, constitutive material descriptions). However, advanced variants of FEM are required in order to avoid mesh tangling and distortion when the interaction between various deformable or rigid bodies is included.

One such advanced variant is the Particle Finite Element Method (PFEM), which is here employed to simulate the screw piles in clayey soil. The work is structured as follows: first, the numerical method is outlined; after presenting a validation analysis (the simulation of the insertion of a pile) some preliminary results are highlighted; finally, some conclusions are drawn.

NUMERICAL MODEL

The Particle Finite Element Method is characterized by a particle discretization of the domain: every time step a finite element mesh – whose nodes are the particles – is constructed using a Delaunay's tessellation and the solution is evaluated using this mesh with well-shaped, low-order elements. The continuum is modeled using an Updated Lagrangian formulation^{3,4}. Additionally, *h*-adaptive routines are employed to obtain a better discretization of the domain. New particles are introduced in areas where large plastic dissipation is generated. These zones must be refined because the number of particles may become too low to obtain an accurate solution. On the contrary, due to high shear deformations, particles may locally concentrate in the same region of the domain. To overcome the difficulties that may follow from that, particles that are closer than a characteristic distance are removed.

Numerical simulations have been carried out by means of the numerical code G-PFEM⁵, specially developed for the analysis of large strain contact problems in geomechanics. The code is able to accurately simulate the interaction between fluid-saturated porous media and rigid structures using low-order elements for efficiency. Techniques to alleviate volumetric locking are required: in this work, a mixed stabilized formulation⁶. The code is capable of handling coupled problems within quasi-static⁷ or fully dynamic settings⁸. However, in this preliminary study only a relatively simple axisymmetric undrained total-stress model is employed. This approach is reasonable, as the loading of piles in clayey soils occurs at a relatively high velocity compared with the hydraulic properties of clay and undrained conditions prevail.

Model set-up

All the numerical simulations reported in this work share the same constitutive parameters. The soil is assumed to obey a Tresca yield criterion and a quasi-incompressible elastic model, with a Young modulus $E = 2980$ kPa, Poisson's ratio $\nu = 0.49$ and undrained shear strength $S_u = 10$ kPa, which results in a rigidity index of $I_r = G/S_u = 100$.

The pile is considered completely rigid; this hypothesis is approximate enough due to the high ratio between the pile Young's modulus and that of the soil. The contact constraints are imposed in the solution using a Penalty Method. This includes an inbuilt tension cut-off, since no tensions are allowed at the soil-structure interface. The tangential part of the contact is modelled employing the so-called elastic-plastic analogy and, as customary in total stress analyses, the maximum allowable contact tangential stress is taken as a fraction α of the undrained shear strength of the soil.

At the beginning of the simulations, the pile is wished-in-place; thus, installation effects are not considered here. The soil initial state is characterized by a total pressure equal to $p = 200$ kPa and null deviatoric stresses $q = 0$ ($K_0 = 1$). Therefore, at the top boundary a load of 200 kPa is applied. Both displacement components are restricted at the bottom boundary, whereas only the horizontal component is imposed at the vertical boundaries.

Validation analysis: penetration of a simple pile

To showcase the possibilities of the method, results of the penetration of a pile are first presented. Two different cases are presented, one assuming a completely smooth interface and the other with an adhesion equal to half the undrained strength or $\alpha = 0.5$.

Figure 1 presents the main result of interest, namely the bearing capacity factor, N_c , defined as:

$$N_c = \frac{q^{tip} - \sigma_{v0}}{S_u}$$

where q^{tip} is the total tip force divided by the projected area of the pile whereas σ_{v0} stands for the initial total vertical stress. It is clear that after a normalized penetration of one radii, both

cases reach a stationary state. Little influence of the contact roughness is visible in the results: for the smooth case, the mean bearing capacity factor is 8.97 whereas a value of 9.33 is obtained for the rough case. The obtained end bearing capacity factor assuming a smooth interface, $N_c = 8.97$, is in very close agreement with the traditional value proposed by Skempton⁹, $N_c = 9$. Figure 2 illustrates for the smooth case how the failure mechanism accompanies the pile, by plotting incremental plastic shear strain at several penetration depths (ranging from 1 to 5 radii).

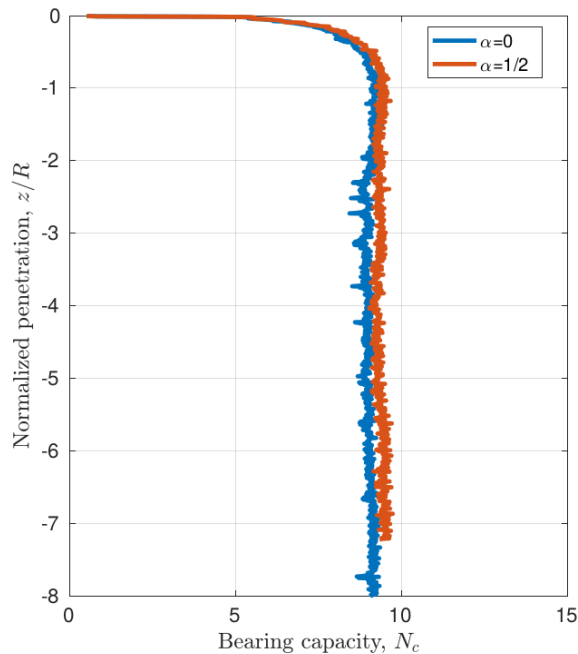


Figure { SEQ Figure * ARABIC }: Closed-ended pile. Normalized penetration curve for the smooth and rough cases.

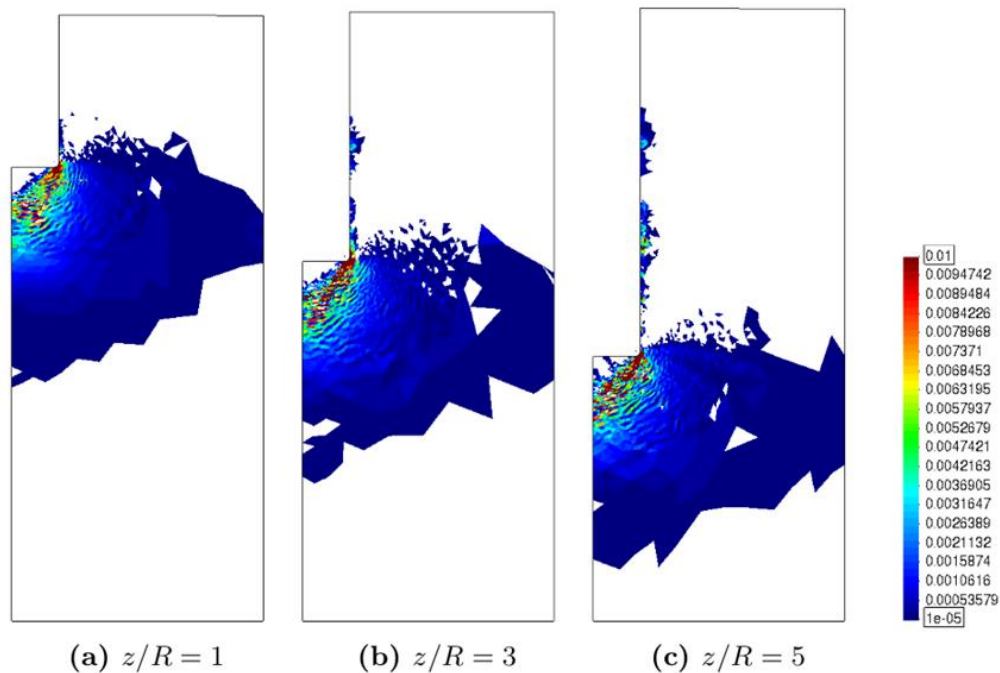


Figure { SEQ Figure * ARABIC }: Closed-ended pile. Smooth interface. Incremental plastic shear strain.

RESULTS AND DISCUSSION

Once the accuracy of the developed numerical framework has been demonstrated, screw piles may be confidently simulated. Two different geometries are assessed with one and two helices (see Figure 3). In both cases a pull-out vertical displacement equal to 0.5 times the radius of the pile is imposed at the head of the pile.

Figure 4 reports the load-displacement curves, where the pile displacement has been normalized by the radius of the pile whereas the load is normalized by the projected area of the pile. At zero displacement a pressure of 200 kPa has to be supplied to neutralize the effect of the initial stress state. For the single helix case, the pile rapidly reaches a steady state with a limit resistance of around 240 kPa. Meanwhile, for two helices, the limit resistance is around 450 kPa with slower resistance mobilization. Three different bearing capacity factors are also presented: for the tip of the pile (introduced previously), and for each individual helix, (defined as the total vertical force acting on their surfaces divided by the projected area and normalized by S_u). Bearing capacity at the tip is negative; in contrast to the analysis of pile penetration the soil fails in an inverse mode. In the pile that only has one helix, the bearing capacity factor of the helix is close to 12. In contrast, in the case with two helices this capacity factor is of around 9.

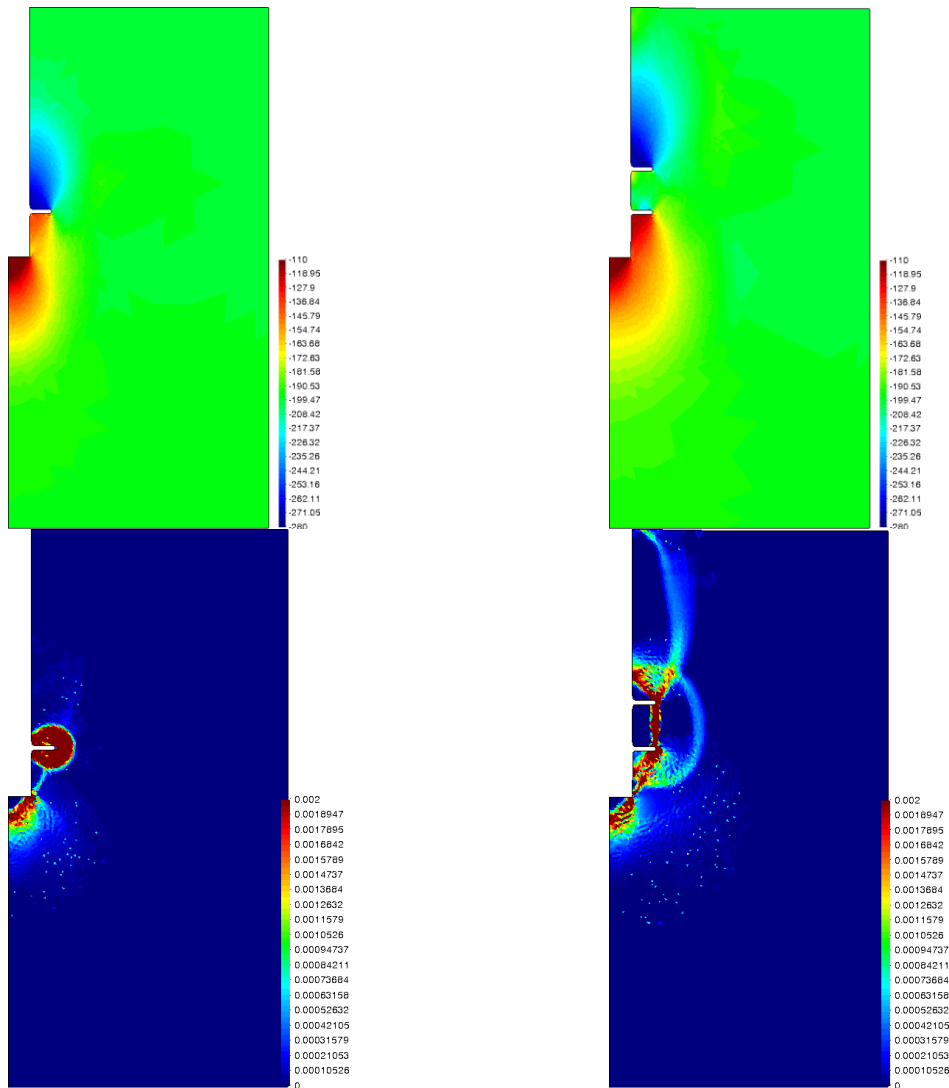


Figure 3: Total vertical stress [in kPa] (top) and incremental plastic shear strain (bottom) for cases with one (left) and two helices (right)

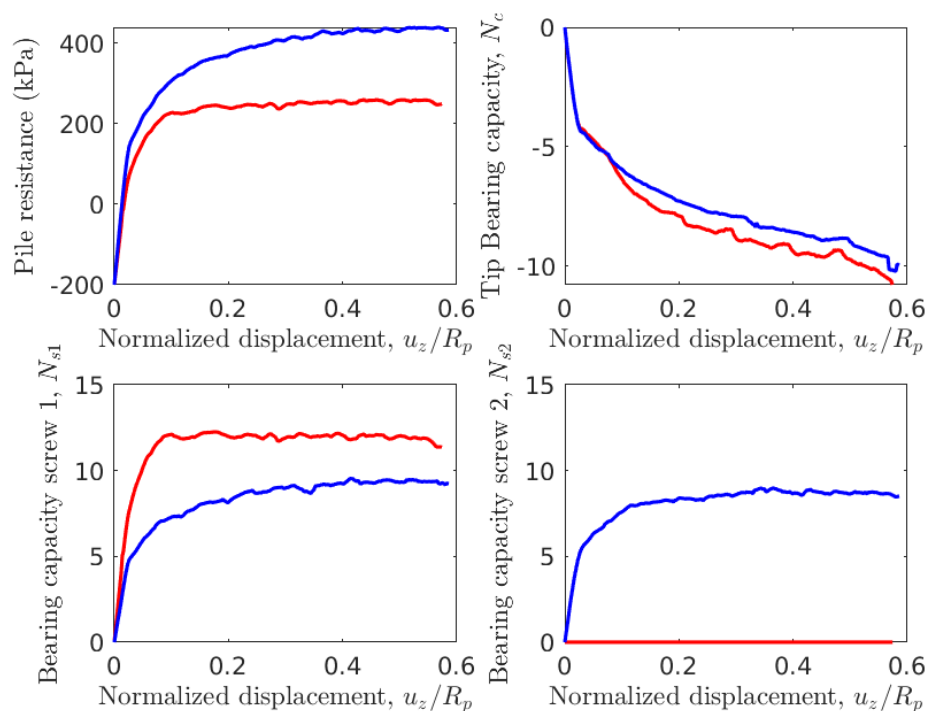


Figure 4: Evolution of the pile resistance, tip bearing capacity and bearing capacity factor of each screw in terms of the normalized uplift. Results for the geometry with two plates are depicted in blue.

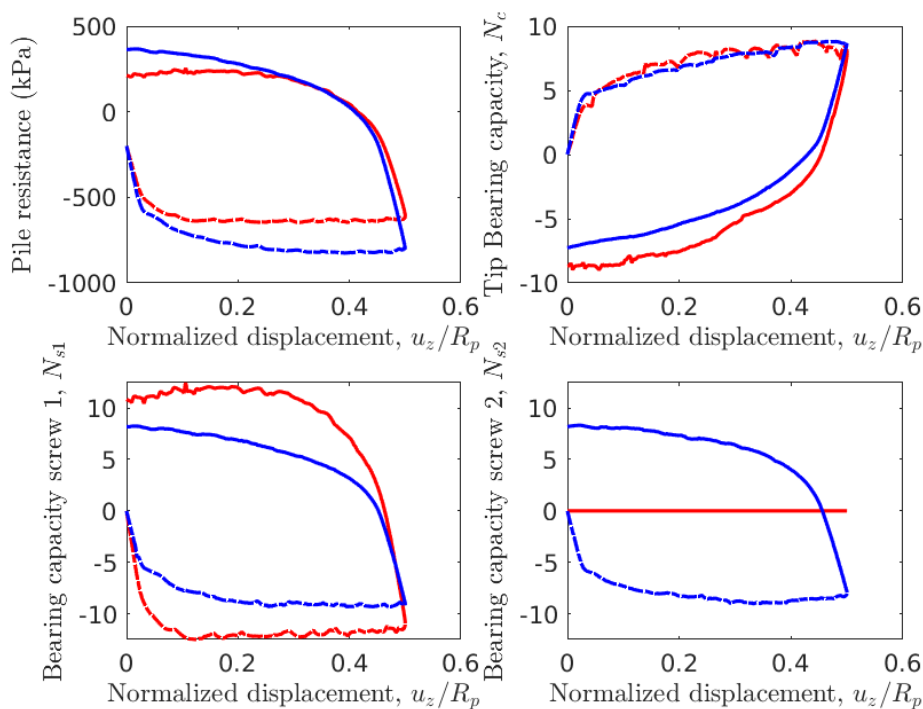


Figure 5: Push-pull sequence. Evolution of the pile resistance, tip bearing capacity and bearing capacity factors. Results for two plates are depicted in blue. Results during the penetration phase are plotted with a discontinuous line

In both cases (Figure 3) the vertical stress (negative in compression) is reduced below the tip of the pile, whereas it is in high compression above the upper helix. Interestingly, no large variations in the stress field appear in the region between the two helices. Also, due to the moderately high initial stress (200 kPa), all the soil remains in contact with the structure during pull-out. Figure 3 also reports incremental plastic shear strain, to give an indication of the failure

mechanism. With two helices, a cylinder-shape failure mechanism is observed between both helical plates, since they are relatively close to each other ($2R$). For a single helix, a flow-around mechanism is obtained. Finally, another set of simulations was run in a first approximation to installation effects. This time, first, the pile is penetrated $0.5R$ and then pulled out by the same amount. Figure 5 presents load-displacement curves, where the penetration phase is depicted with discontinuous lines and the subsequent pulling test with a continuous line. No large discrepancies from the previous result are observed for the pulling phase.

CONCLUSION

This contribution has outlined preliminary results of the numerical simulation of screw pile pull-out by means of the Particle Finite Element method. In particular, the effect of the number of helical plates has been assessed. Details of the total resistance and also the failure mechanism have been shown. The developed numerical scheme appears to be a promising tool for the simulation of tool-soil interaction.

ACKNOWLEDGEMENT

This research was partly funded by the Spanish MEC through grant BIA2017-84752-R

REFERENCES

1. Wang, D., Merifield, R. S: and Gaudin, C. Uplift behavior of helical anchors in clay. *Canadian Geotechnical Journal*, 50: 575-584 (2013).
2. Al-Baghdadi, T. Screw piles as offshore foundations. Numerical and physical modelling. PhD Thesis (University of Dundee) (2018)
3. Oñate, E., Idelsohn, S.R., Del Pin, F. & Aubry, R. The Particle Finite Element Method – an overview. *International Journal of Computational Methods* 1(2) 267-307 (2004).
4. Rodriguez, J.M., Carbonell, J.M., Cante, J.C. & Oliver, J. The Particle Finite Element Method (PFEM) in thermo-mechanical problems. *Int. J. for Numerical Methods in Engineering*, 107(9): 733-785 (2016).
5. Monforte, L., Arroyo, M., Carbonell, J.M. & Gens, A. Numerical simulation of undrained insertion problems in geotechnical engineering with the particle finite element method (PFEM). *Computers and Geotechnics*. 82, 144-156 (2017).
6. Monforte, L., Carbonell, J.M., Arroyo, M. & Gens, A. Performance of mixed formulations for the particle finite element method in soil mechanics problems. *Computational Particle Mechanics*. 4(3), 269-284 (2017).
7. Monforte, L., Arroyo, M., Carbonell, J. M., & Gens, A. (2018). Coupled effective stress analysis of insertion problems in geotechnics with the Particle Finite Element Method. *Computers and Geotechnics*, 101, 114-129.
8. Monforte, L., Navas, P., Carbonell, J. M., Arroyo, M., & Gens, A. (2019). Low- order stabilized finite element for the full Biot formulation in soil mechanics at finite strain. *Int. J. for Numerical and Analytical Methods in Geomechanics*, 43(7), 1488-1515.
9. Skempton, A. W. The Bearing capacity of clays. *Building Research Congress, London, The Institution of Civil Engineering*, 180-189 (1951).